Mexican jumping beans exhibit diffusive motion

Devon McKee and A. Pasha Tabatabai

Phys. Rev. E **107**, 014609 — Published 25 January 2023

DOI: 10.1103/PhysRevE.107.014609

Mexican jumping beans exhibit diffusive motion

Devon McKee and A. Pasha Tabatabai[*]
Department of Physics, Seattle University, Seattle, WA, USA

Organisms across many lengthscales generate specific strategies for motion that are crucial to their survival. Here, we detail the motion of a non-traditional organism, the Mexican jumping bean, where a larva encapsulated within a seed blindly moves the seed in search of shade. Using image analysis techniques, we quantitatively describe the motion of these objects as active particles. From this experimental data, we build a computational simulation that quantitatively captures the motion of these beans. And we further evaluate the effectiveness of using the observed diffusive strategy to find shade, suggesting that the random walk is an advantageous strategy for survival.

I. INTRODUCTION

All living organisms utilize chemical energy to propel themselves. For example, many flagellated bacteria at the micro-meter scale undergo run and tumble motion, with ballistic trajectories intermixed with randomizing tumbles [1]. At significantly larger lengthscales, migratory birds and mammals travel long distances before significantly changing course [2, 3]. Thus, the characteristics of motion for organisms are varied; there is no unique strategy for motion.

There are plenty of efforts to describe the wide range of motile behaviors of organisms and to use these behaviors to define rules [4] or engineer synthetic systems [5, 6]. For example, Janus colloids [7–9] that move across a chemical potential capture some features of bacterial motion. Characterizing these motions of isolated individuals is a precursor to studying the non-trivial influencing effects of groups [10, 11].

In this paper, we investigate the motile behavior of a non-traditional organism: the so called Mexican jumping bean. This colloquial name is a misnomer, as the 'bean' is actually a moth larva (*Laspeyresia saltitans*) confined within the seed of a spurge tree (*Sebastiania pavoniana*) native to Mexico [12]; multiple varieties of jumping bean exist [13]. These larva feed off the inside of the seed until they eventually pupate and leave the seed. Within their native habitat, these jumping beans lay on the desert floor and must periodically move out of the direct sunlight and into the shade of a tree to survive. Internal thrusting of the larva [14] results in small bean jumps. Previous work has been done to identify temperatures that initiate jumping [15] as well as classify jumping methods and qualitatively describe motion in temperature gradients with applications for robotics [14].

Here, we use image analysis techniques to quantitatively describe the statistical behaviors of the motion of these beans in the absence of thermal gradients and find that motion follows a random walk. We also build a computational simulation that quantitatively recreates bean motion. Further, we consider the search for shade as a first-passage problem, which motivates the evolutionary advantage of diffusive motion for bean survival.

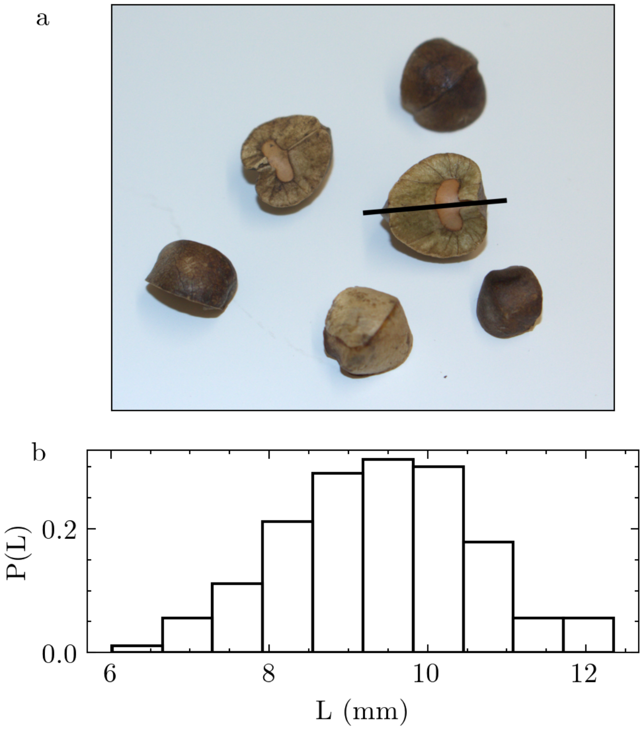

FIG. 1. Bean Size Distribution. (a) Photograph of six beans of various sizes resting on a 2D surface on their different faces - two on their curved edge and four on a flat face. A line is displayed to define where the pole-pole length L is measured for a bean. (b) Probability distribution of bean lengths $P(L)$ for $N = 142$ beans.

II. BEAN DETAILS

Mexican jumping beans are purchased from a commercial supplier (www.amazingbeans.com) and stored at room temperature in individual containers. The shapes of these beans are akin to wedges made from cutting a sphere into thirds along longitudinal lines from pole-to-pole. (Figure 1a) [14]. To define a characteristic size for each bean, we measure the pole-to-pole distance L, which

---

[*] tabatabai@seattleu.edu

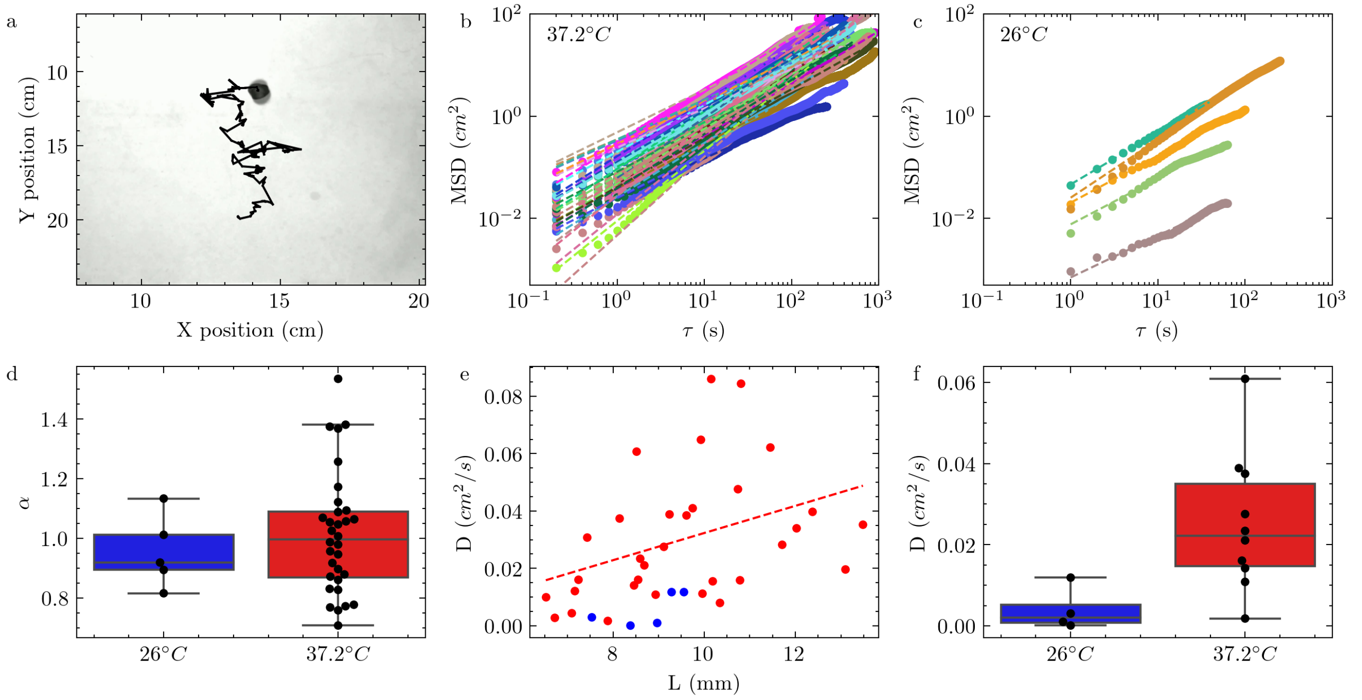

FIG. 2. Effective Diffusion Constant is Size Dependent. (a) Example of experimental data with photograph of bean overlaid with bean trajectory over time. (b) Mean squared displacement MSD as a function of lag time τ for $N = 32$ beans at a temperature of 37.2 ± 1.5 °C. Each set of markers corresponds to experimental data for a given bean, and lines are best fits. (c) MSD as a function of τ for $N = 5$ beans at 26 ± 3 °C. (d) Scaling parameter α for beans at 26 °C and 37.2 °C. Two-sided Students t-test gives $p > 0.05$. (e) Effective diffusion constant D as a function of bean size L for beans at 37.2 ± 1.5 °C (red symbols) and beans at 26 ± 3 °C (blue symbols), with line of best fit ($p < 0.01$) calculated only for beans at 37.2 ± 1.5 °C. (f) Effective diffusion constant for beans with 7.5mm $< L <$ 9.5mm at 26 °C and 37.2 °C. Two-sided Students t-test gives $p < 0.05$. All data points used in generating box plots in (d,f) are overlaid atop respective box plot.

is also an approximation for the diameter for the three-seed arrangement. We find $L = 9.4 \pm 1.2$ mm (mean ± std.) (Figure 1b).

Heckrotte showed that the environmental temperature plays a significant role in the activity of the jumping bean [15]. Beans within the range of 20°C-35°C had equivalent durations of activity, whereas higher or lower temperatures decreased the amount of activity significantly. Within these active windows, higher temperatures led monotonically to more movements per unit time. As such, we performed our study with a primary temperature of 37.2 ± 1.5 °C ($N = 32$ beans) to maximize the overall activity of the bean as well as the number of jumps within an active window. In addition, we provide measurements at a temperature of 26 ± 3 °C ($N = 5$ beans) to investigate the effects of temperature on motion.

It has been previously shown that the non symmetric shape of the bean leads to multiple unique modes of motion [14]. While little is known about the connection between motile strategies, larva size, and relative larval orientation within the bean, West et al. defined the observed modes of bean motion as flipping, rolling, and jumping. At room temperature, high-speed images showed that jumping modes where the bean begins and ends with the same surface on the ground are most frequent and represent 87% of all events. With such a large bias towards jumping events, we choose to record all motile steps in our study as changes in bean position, regardless of maneuver type.

III. RESULTS

Individual beans are placed on a flat 2D surface that is held at a uniform temperature. A temperature-controlled recording stage for imaging was built from electrically heated mats and topped by an aluminum sheet for even heat dispersal; temperature is measured by an infrared thermometer. Diffused photographic lamps are used to illuminate the recording stage from above, and lighting is kept constant for all beans to avoid potential light intensity dependent effects. A sheet of standard 8.5in×11in white paper is placed atop the aluminum sheet for image contrast.

At these conditions, beans are motile (Supplementary Video 1) [14, 15], and we use a Pixelink PL-D7620 machine vision camera at frame rates between 1-5 frames per second for a total of 5-60 minutes to collect position data for 37 beans equivalent to approximately 37

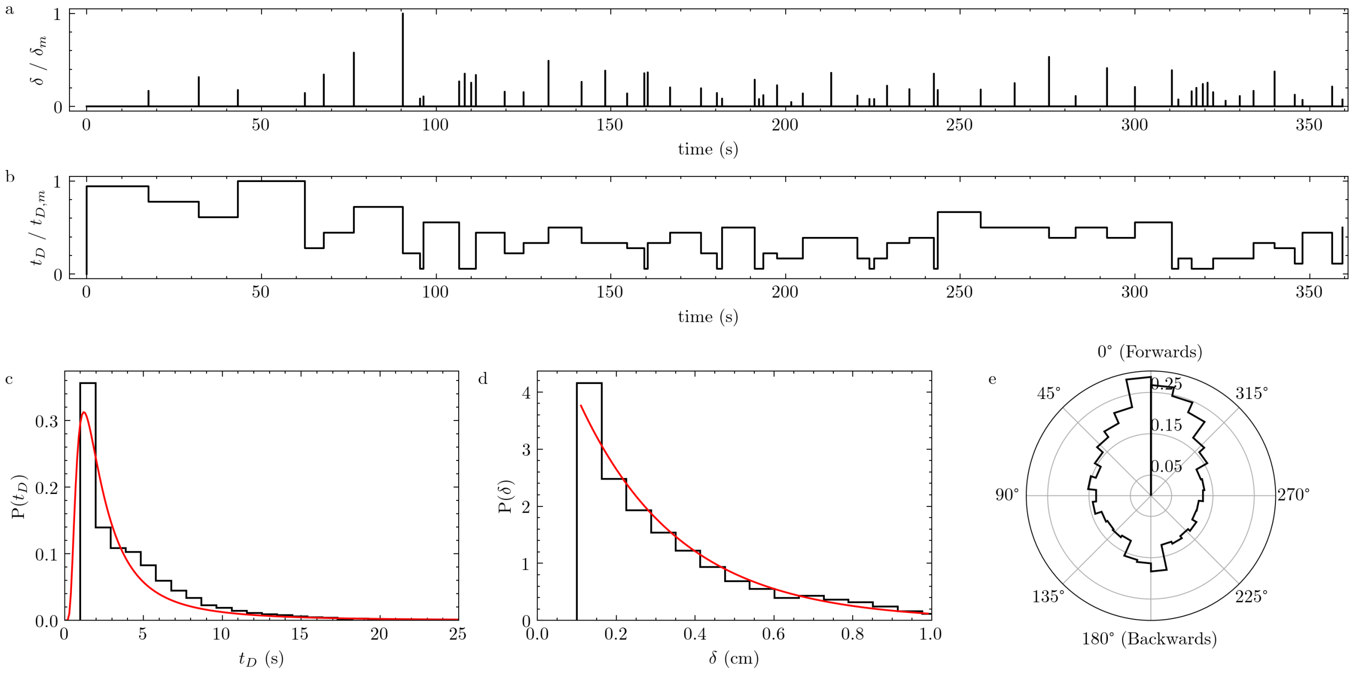

FIG. 3. Step Details of Bean Motion. (a) Example of displacement δ normalized by maximum displacement δ_m and (b) delay t_D normalized by maximum delay $t_{D,m}$ for a single bean over 10 minutes. (c) Probability distribution of delay t_D with fitted inverse gamma distribution. (d) Probability distribution of displacement δ with fitted exponential distribution. (e) Probability distribution of relative angular displacement where $\theta = 0$ degrees are forward jumps. Data shown in (c-e) are aggregated over all $N = 32$ beans at 37.2 ± 1.5 °C and each contain ~ 9300 total steps.

hours of video [16]. The maximum continuous trajectory for each bean is set by the time it takes for a bean to wander off of the imaging stage (Supplementary Movie 1). When this happens, beans are returned to the center of the imaging area, and further motion contributes to the ensemble statistics of that particular bean. Frames are captured as grayscale images, and image preprocessing steps include heightening of image contrast and a perspective transformation to account for camera skew. During processing, bean position is determined by image thresholding, contour calculations, and centroid calculations. Pixel positions are converted into real-space positions using the known dimensions of the 8.5in×11in paper. Preprocessing, processing, and image transformations were performed using Python and the computer vision library OpenCV. Further position data processing, analysis, and plotting were performed using the Python plotting library Matplotlib. All code is available on GitHub (https://github.com/tablabsu/cydia-saltitans).

These image analysis techniques yield bean position $\vec{r}$ and the 2D trajectories $\vec{r}(t)$ over time t (Figure 2a). Using $\vec{r}(t)$, we calculate the mean squared displacement MSD for each bean $\left\langle(\vec{r}(t+\tau)-\vec{r}(t))^2\right\rangle$ as a function of lag time τ (Figure 2b). We find that $\left\langle(\vec{r}(t+\tau)-\vec{r}(t))^2\right\rangle \sim \tau^\alpha$ with $\alpha = 1.0 \pm 0.2$ (mean ± std.) for $N = 32$ beans at 37.2 ± 1.5 °C (Figure 2d). As such, we conclude that the average bean behavior is to undergo a random walk. This α scaling is constant across all values of τ, which is in contrast to the previous qualitative observation of 'run-and-tumble' type motion in the presence of a thermal gradient [14].

For comparison, we also measure the MSD for beans held at a lower temperature of 26 ± 3 °C (Figure 2c). These beans also exhibit diffusive motion with $\alpha = 0.95 \pm 0.12$ (mean ± std.) (Figure 2d). Using the two-sided Students t-test with unequal variance, these α distributions are not statistically different. Therefore, we conclude that temperature does not influence the motile strategy of these beans; motion is diffusive for each of these experimental temperatures.

Given that beans are undergoing a random walk, we then use the 2D MSD to define a non-thermal effective diffusion constant D found through the expression $\left\langle(\vec{r}(t+\tau)-\vec{r}(t))^2\right\rangle = 4D\tau$. Surprisingly, we find a relationship between D and bean size L; D increases with L (Figure 2e). Interestingly, this relationship is in contrast to the size dependent diffusion constant for thermally diffusing particles given by the Stokes-Einstein relation [17]. We observe significant spread in the relationship between D and L, which may be a consequence of possible variations in larva size within the bean. Or this could be a result of defining D for the few beans where α is furthest from unity.

In addition, we make a direct comparison between D for measurements made at 26 °C and 37.2 °C. Since we found D to be size dependent, we partition the data and look only at the effective diffusion constants for beans of equivalent size. D for beans with pole-to-pole length 7.5mm $< L <$ 9.5mm, chosen to match the size range of beans measured at 26 °C, are statistically different across the different temperatures (Figure 2f). Therefore, while beans utilize diffusive motion at different temperatures, their effective diffusion constant appears to be temperature dependent.

While the scaling of the MSD reveals the type of motion (ex: $\alpha = 1$ for diffusive motion versus $\alpha = 2$ for ballistic motion), it does not provide information about the discrete steps associated with motion. As such, we investigate these discrete jumps using three separate metrics and the definitions that 1) consecutive jumps are separated by at least one second - a detail that is rooted in visual observations, and 2) a jump must move the bean center-of-mass by at least 1.0 mm. These two assumptions help to distinguish discrete jumps from artifacts associated with capturing imaging frames mid jump. Furthermore, we do not distinguish between the different types of jumps (i.e. rolls, jumps, and flips) that have previously been defined [14].

We quantify motion by defining a displacement δ for each jump as well as a delay time between consecutive jumps t_D. We observe jumps with heterogeneous jump sizes as well as sporadic intervals between each jump (Figure 3a,b). By aggregating the data for all beans at 37.2 °C, we build probability distributions for δ and t_D. Aside from an increase in probability of large δ for large beans (Supplementary Figures 1 & 2), consistent with Figure 2e, we notice that the distributions of τ_D and δ are qualitatively similar across bean sizes.

We observe that almost all jumps occur within ten seconds (Figure 3c). This distribution is reminiscent of a Lévy distribution describing random processes, consistent with these jumps occurring seemingly at random. This is a special case of the inverse gamma distribution, and we fit the distribution of τ_D to the inverse gamma distribution with shape and scale constants equal to 1.75 and 3.6, respectively.

The distribution of δ reveals that most jumps are small (2-3 mm), though the probability of finding large jumps approximately equal to the average bean size ($\delta \sim \langle L \rangle$) is non-zero (Figure 3d). This distribution is fit to an exponential function and has a decay constant of 0.3 cm. The shape of this distribution of jump sizes is consistent with the relative sizes and frequencies of previously measured modes of motion at room temperature, albeit at lower values of jump size [14].

In addition, we examine the change in angular displacement between subsequent jumps. We define $\theta = 0°$ for forward motion (i.e. no change in direction between jumps) and $\theta = 180°$ for backwards motion (i.e. the bean reverses direction) (Figure 3e). In general, the distribution of jump angles has a slight tendency towards continuing forward or reversing direction as opposed to turning left or right (90°/270°).

In all, we have quantitatively measured the details for each individual step across all beans and have best-fit functions that approximate the distributions of τ_D and δ.

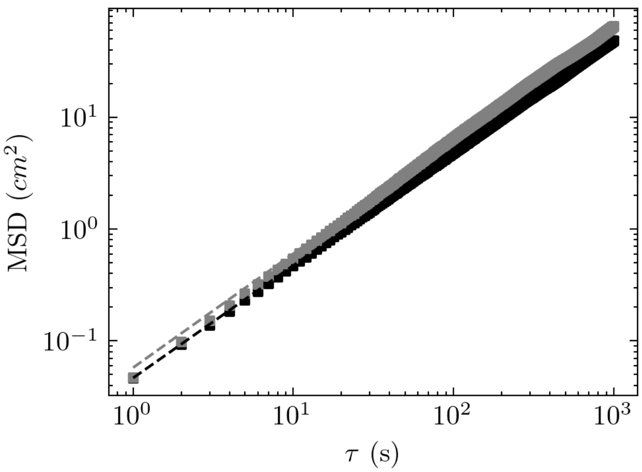

FIG. 4. Simulated Bean Motion. Mean squared displacement MSD as a function of lag time τ of simulation trajectories with an isotropic (black) angular distribution and a distribution directly sampled from experimental data in Figure 3e (gray). Dashed lines are lines of best fit for MSD $\sim \tau^{\alpha}$ with α = 1.01 and α = 1.02 for the isotropic and experimental angular distributions, respectively.

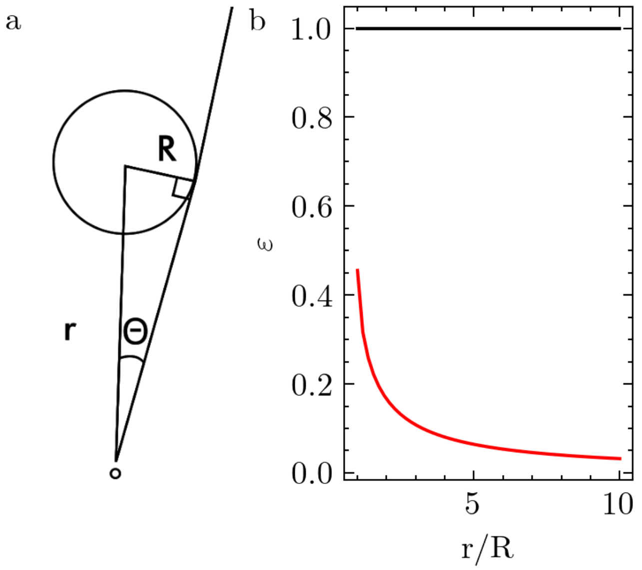

FIG. 5. First-passage to shade. (a) Schematic of circle with radius R denoting shade and an object at initial position $r > R$ away from the shade. (b) Eventual hitting probability ε as a function of object initial position r/R for diffusive objects (black) and ballistic objects (red).

We observe through the MSD measurement that motion is diffusive (Figure 2). However, the distribution of angles has a slight bias towards forward motion, which is not consistent with diffusive motion (Figure 3). To explore this potential conflict, we perform numerical simulations of bean motion. These simulations of a single isolated particle undergoing a random walk use the fitted distributions of experimentally measured displacements and delay times from Figure 3. However, one simulation samples from an isotropic angular distribution, whereas the other simulation samples directly from the experimentally measured angular distribution in Figure 3e. By controlling the details of each jump, we measure the simulated bean position $\vec{r}(t)$ and the subsequent MSD. We observe very little difference between these two results (Figure 4); both have $\alpha \sim 1$ which matches the experimentally observed α values. Therefore, we conclude that our measurements are consistent.

Furthermore, we measure effective diffusion constants $D = 0.0196$ cm^2/s and $D = 0.0163$ cm^2/s using the isotropic angular distribution and experimentally measured angular distribution, respectively. These values are consistent with the range of individually measured effective diffusion constants.

IV. DISCUSSION

We have presented a detailed characterization of Mexican jumping bean motion where beans are shown to undergo a random walk. We confirm that these results are robust to changes in friction between the bean and the 2D surface (Supplementary Figures 3-5). We find that the diffusion constant for larger beans is higher than for small beans, in contrast to thermally diffusing particles; we do not have any information on the sizes of the larva within each bean, which may be a cause for the large spread in data within Figure 2e. Using this experimental data, we create a simulation that captures the diffusive behavior of bean motion.

At first glance it may appear that a diffusive strategy for these animals to escape direct sunlight would be ineffective. To explore this further, we compare diffusive and ballistic strategies for finding shade as a first-passage problem. Let's assume that the shade from a tree is a circle with radius R and that a bean is within the sun at a position $r > R$ and free to move in 2D (Figure 5a). For an object undergoing diffusive motion, the eventual hitting probability $\varepsilon = 1$ regardless of starting position [18]. Now consider a ballistic object with a randomly chosen starting orientation. The maximum angle that will lead to an eventual hit is the grazing incidence depicted in Figure 5a. Therefore, the eventual hitting probability is the ratio of this angle subtended by shade to the 2D solid angle $\varepsilon(r) = \frac{1}{\pi}\sin^{-1}(R/r)$ (Figure 5b). Therefore, only a small fraction of ballistic objects, but all diffusive objects, will find shade. Those ballistic objects that do find shade, will find shade faster than the diffusive objects. Note: in practice, the first-passage time for some diffusive objects will be greater than the lifetime of a bean. These results suggest that diffusive motion in Mexican jumping beans does not optimize for finding shade quickly. Rather, Mexican jumping beans use a strategy that minimizes the chances of never finding shade when shade is sparse.

---

[1] H. C. Berg, *E. coli in motion* (Springer, New York, 2004).

[2] R. Kays, M. C. Crofoot, W. Jetz, and M. Wikelski, Science **348**, 10.1126/science.aaa2478 (2015).

[3] C. J. Torney, M. Lamont, L. Debell, R. J. Angohiatok, L.-M. Leclerc, and A. M. Berdahl, Philosophical Transactions of the Royal Society B: Biological Sciences **373**, 20170385 (2018).

[4] P. Romanczuk, M. Bär, W. Ebeling, B. Lindner, and L. Schimansky-Geier, The European Physical Journal Special Topics **202**, 1 (2012).

[5] M. M. Genkin, A. Sokolov, O. D. Lavrentovich, and I. S. Aranson, Physical Review X **7**, 011029 (2017).

[6] F. J. Sevilla and M. Sandoval, Physical Review E **91**, 052150 (2015).

[7] S. C. Glotzer and M. J. Solomon, Nature Materials **6**, 557 (2007).

[8] H. Karani, G. E. Pradillo, and P. M. Vlahovska, Physical Review Letters **123**, 208002 (2019).

[9] H.-R. Jiang, N. Yoshinaga, and M. Sano, Physical Review Letters **105**, 268302 (2010).

[10] T. Vicsek, A. Czirók, E. Ben-Jacob, I. Cohen, and O. Shochet, Physical Review Letters **75**, 1226 (1995).

[11] A. Berdahl, C. J. Torney, C. C. Ioannou, J. J. Faria, and I. D. Couzin, Science **339**, 574 (2013).

[12] In taxonomic references, the moth is referred to by various names, the most common being *Laspeyresia saltitans*, *Cydia saltitans* and *Cydia deshaisiana*. In this paper, we select the name appearing most often in referenced literature.

[13] The authors are aware of the larva *Emporia melanobasis* which inhabits the seeds of the Tamboti tree *Spirostachys africana* in South Africa.

[14] D. M. West, I. K Lal, M. J. Leamy, and D. L. Hu, Bioinspiration & Biomimetics **7**, 036014 (2012).

[15] C. Heckrotte, Journal of Thermal Biology **8**, 333 (1983).

[16] See Supplemental Material at [URL will be inserted by publisher] for Supplemental Figures and Videos.

[17] P. M. Chaikin and T. C. Lubensky, *Principles of Condensed Matter Physics* (Cambridge University Press, Cambridge, 2000).

[18] S. Redner, *A guide to first-passage processes* (Cambridge University Press, Cambridge, 2008).